Identifying Energy Extraction Optimisation Strategies of *A. succinogenes*

By

Waldo G. Lexow

A dissertation presented in the fulfilment of

the requirements for the degree of

Master of Science

in

Chemical Technology

Supervised by Prof. W. Nicol

at the

Division of Bioreaction Engineering, Department of Chemical Engineering

Faculty of Engineering, the Built Environment and Information Technology

University of Pretoria

Pretoria

December 2019

Synopsis

Actinobacillus succinogenes is known to produce the acids of acetate and formate as co-products in conjunction with succinic acid. These compounds not only divert a portion of the carbon flux away from succinic acid production, but also necessitate separation techniques that further augment production costs and, as a result, render the bio-production of succinic acid unviable. To explore methods of reducing or eliminating the production of these co-products, one needs to understand the reason for their presence in the first place. This study aimed at defining the energy boundaries that describe the fermentative behaviour of the microbe.

It was found that *A. succinogenes* displays a clear preference for routes with higher energy extraction efficiency in the early stages of its batch-operated lifespan, subsequently replacing the routes with others of lesser efficiency as fermentation progresses. This clear observation of diminishing energy extraction efficiency supports the idea of route hierarchy, i.e. routes that are more efficient at extracting energy from the available resources are favoured over those that are less efficient. Furthermore, it suggests that accumulated environmental stresses is a likely reason for the observed shift in metabolic strategies for energy extraction. This idea is further supported by the finding of co-activation between the pyruvate dehydrogenase and pyruvic acid excretion routes. Since these have vastly different energy extraction capabilities, it is postulated that the pyruvic excretory pathway is an inherent overflow response mechanism activated to limit the amount or rate of acetic acid production. This suggests a scenario in which the co-production of pyruvic acid is holistically energetically more favourable. The prevailing postulate is that the build-up of acetic acid (and formic acid), if left unchecked, might result in a runaway energy cost effect. By limiting the external pressure of passive back-diffusion, the organism is in an energetically more favourable position since less energy need be wasted on the active export of those components.

Acknowledgements

I wish to acknowledge with gratitude the following individuals:

My supervisor, Prof. W. Nicol, for his intellectual and financial support as well as the time he invested in the undertaking of this project.

Dr HG Brink for his outstanding role as co-supervisor and his assistance throughout the duration of my time as a Master's student at the BRX labs.

My colleagues, Dr S Mokwatlo & Mrs M Geyer-Johnson, for all their extensive help and continued friendship.

My parents, Marlene and Theo Lexow, for their endless faith in my capabilities, and their encouragement and support.

The financial assistance of the National Research Foundation (NRF) towards this research is hereby acknowledged. Opinions expressed and conclusions arrived at are those of the author and are not necessarily to be attributed to the NRF.

Contents

List of Figures

List of Tables

Nomenclature

3PG	3-Phosphglycerate
Ace	Acetic acid
AceCoA	Acetyl Coenzyme A
ADP	Adenosine Di-Phosphate
ATP	Adenosine Tri-Phosphate
CSL	Corn Steep Liquor
DCW	Dry Cell Weight
Dex	Dextrose
E4P	Erythrose-4-Phosphate
EMP	Embden–Meyerhof–Parnas
ETC	Electron Transport Chain
EtOH	Ethanol
ETP	Electron Transport-Coupled Phosphorilisation
F6P	Fructose-6-Phosphate
FDH	Formate Dehydrogenase
FDP	Fructose-1,6-Di-Phosphate
For	Formic acid
Fum	Fumaric acid
G3P	Glyceraldehyde-3-Phosphate
G6P	Glucose-6-Phosphate
HPLC	High-Performance Liquid Chromatography

Mal	Malic acid
NAD(H)	(Dihydro)Nicotinamide Adenine Dinucleotide
NADP(H)	(Dihydro)Nicotinamide Adenine Dinucleotide Phosphate
OD_{660}	Optical Density as measured at 660 nm
OPPP	Oxidative Pentose Phosphate Pathway
ORP	Oxidoreduction potential
Oxa	Oxaloacetic acid
Δp	Transmembrane Proton Gradient
PDH	Pyruvate Dehydrogenase
PEP	Phosphoenolpyruvate
PFL	Pyruvate Formate Lyase
PMF	Proton Motive Force
Pyr	Pyruvic acid
Ru5P	Ribulose-5-Phosphate
SLP	Substrate Level Phosphorylation
Suc	Succinic acid
TeA	Terminal electron Acceptor
TCA	Tricarboxcilic acid
TSB	Tryptic Soy Broth
vvm	Volumetric Flow Rate of Gas per Reactor Volume
YE	Yeast Extract
YNB	Yeast Nitrogen Base without Amino acids

1 Introduction

The production of commodity chemicals from a petroleum-based origin has long been known to be unsustainable. The eventual depletion of the planet's non-renewable crude oil reservoirs is an inevitable eventuality (Shafiee & Topal, 2009). And though the liberal use of the resource catalysed industrialisation, fuelled the technological boom and gave birth to the age of plastic, it also came with an immense environmental cost. Today, however, it is almost impossible to imagine civilisation without the vast array of products derived from this cheap resource. Thus, to future-proof society, over the past few decades global research efforts have focused on switching from this exhaustible natural resource to others which are more sustainable and environmentally accommodating. One such avenue explored is the use of large-scale biorefineries, exploiting the natural processes of microbes and/or enzymes to convert renewable plant-based sugars, obtained from agricultural waste streams, to useful platform chemicals required by industry. On this account, the US Department of Energy (DOE) identified 12 key bio-derivable compounds that would help facilitate the aforementioned shift (Werpy & Petersen, 2004; Bozell & Petersen, 2010).

Succinic acid , one of the identified compounds and the focus of this study, bears remarkable structural similarity to maleic anhydride, a commodity chemical with an industrial

market valued at 2.77 billion USD for 2018 (Grandviewresearch.com, 2019). The four-carbon dicarboxylic acid is readily produced as an intermediate in the TCA cycle of many organisms, and to date several microbes have been identified as possible bio-catalysts for its industrial-scale production. *Mannheimia succiniciproducens* (Lee et al., 2002), *Anaerobiospirillum succiniciproducens* (Lee et al., 2000), *Escherichia coli* (Lin, Bennett & San, 2005), and *Actinobacillus succinogenes* (Guettler, Rumler & Jain, 1999) have all proved to be promising candidates.

A. succinogenes, in particular, has gained significant popularity due to its distinctive ability to produce high concentrations of succinic acid (Zeikus, Jain & Elankovan, 1999) while tolerating high substrate and acid titres (Lin et al., 2008) from a broad range of carbon sources (including arabinose, cellobiose, fructose, galactose, dextrose, lactose, maltose, mannitol, mannose, sorbitol, sucrose and xylose) under anaerobic conditions (Song & Lee, 2006). These properties allow the fermentation of cane molasses, whey and wheat hydrolysates, which are much cheaper carbon sources than refined sugar and dextrose (Beauprez et al., 2010). Furthermore, the bovine rumen bacterium's fermentative production of succinic acid occurs via a reductive TCA pathway, necessitating the incorporation of a molar equivalent of carbon dioxide and thus incentivising the routes' economic and environmental value (McKinlay et al., 2010). However, its reductive pathway also necessitates a net consumption of redox, which is supplied by the organism through the activation of complementary redox producing pathways. These pathways, in the case of *A. succinogenes*, lead to the co-production of acetic, formic and pyruvic acid which not only divert carbon away from succinic acid production, but also augment downstream processing costs. For the bio-based production of succinic acid to become cost-competitive with the current petrochemical production route, aspects such as finding cheaper feedstock (Luthfi et al., 2016) and attaining high succinic acid productivity in high cell density fermentation (Brink & Nicol, 2014) have been studied and reported in the literature. However, the co-production of other fermentation products is still considered to be a key hurdle to the bio-based production economy.

Near-homogeneous production of succinic acid by *A. succinogenes* is theoretically possible when considering the redox producing oxidative pentose phosphate pathway (OPPP) (Bradfield & Nicol, 2016). By liberating half a molar equivalent of carbon dioxide enough redox may be produced to satisfy homogeneous succinate production at a theoretical maximum of

1.124 $g.g^{-1}$ dextrose, due to the capnophilic nature of producing succinic acid utilising a reductive TCA pathway. Although this combination of catabolic pathways is favourable from perspective of succinic acid production, virtually all the literature regarding wild-type *A. succinogenes* fermentation reports on the accumulative presence of formic acid and acetic acid. Moreover, a shift in the acid distribution profile – evident in batch data, and the direct association with the dextrose consumption rate found in continuous production data (Bradfield & Nicol, 2014) – points to an adapting catabolic flux.

For insight into why this occurs, this research aimed to obtain a better understanding of the mechanism behind the organism's fermentative behaviour as it relates to an energy-motivated incentive. For this purpose the flow of mass and redox was analysed by generating high-resolution batch fermentation data on two separate media compositions. This was done utilising a custom-built 2.0 L jacketed bioreactor equipped with an in-line flow cell for the real-time spectrophotometric measurement of cellular biomass accumulation.

Precise mass and redox balances of extracellular metabolite concentration data, obtained via High-Performance Liquid Chromatography (HPLC), revealed an energy maximisation strategy that was played out over the fermentative lifespan of *A. succinogenes* in an isolated batch environment. From viewing the data a media-independent sequence of energy extraction pathways was identified, showing a clear descent in energy extraction efficiency as fermentation progresses. This observation provided two important insights, namely (1) that a fermentation-dependent process was causing attenuation of the energy extraction efficiency of the microbe, and (2) that the organism constantly adapted to the change by utilising its next-best energy extraction pathway to maximise the energy acquired from its available feedstock. If it were not for these fermentation-imposed physical limitations, *A. succinogenes* might well never use the less energetically favourable oxidative pentose phosphate pathway (OPPP) for homosuccinic acid production.

These findings may prove to be invaluable in improving fermenter design and operation for obtaining higher succinic acid yields. Moreover, the development of comprehensive physiological theories will provide insight to aid in genetic alteration strategies for the more effective construction of productive designer microbial catalysts.

2 Literature review

2.1 Energetics of Fumarate Respiration

Energy acquisition and its relay are vital to all living organisms to perform work by way of maintenance, growth and reproduction (Koshland, 2002). Chemotrophic organisms do this by facilitating a perpetual redox environment in which highly energised substrate molecules, such as dextrose, are consistently oxidised to yield reduction power.

The reduction power obtained from these reactions is sequentially transferred to less reduced molecules, releasing potential energy as electrons descend the electro-potential gradient. By controlling the electro-potential descent of the released electrons, catabolic energy relay systems allow cells to capture the leached energy in the bio-available form of adenosine tri-phosphate (ATP). Finally, the electrons are deposited in a terminal electron acceptor (TeA). This process results in product molecules which have a smaller combined Enthalpy (*H)* than the starting molecules, signifying a net loss of energy by the overall reaction, to the benefit of the cell (Willey et al., 2011) (Figure 1).

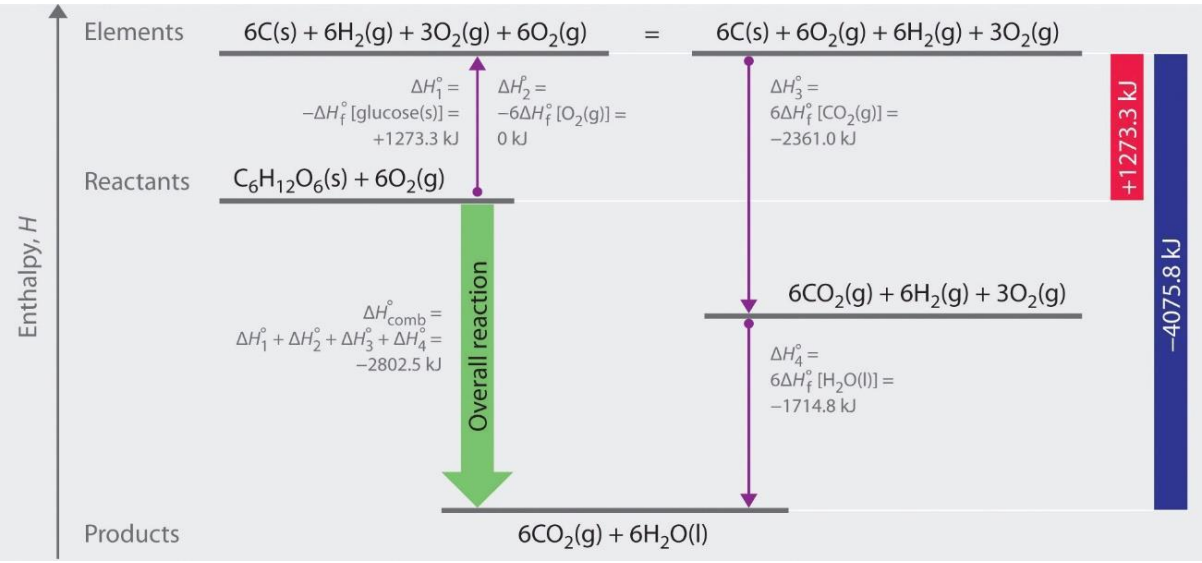

Figure 1: Resulting change in Enthalpy *H* from the combustion of dextrose. Energy released form the overall reaction (green arrow) may be represented as the sum of energy required to separate the reactants (dextrose and oxygen: left) into its elemental constituents (red bar: +1273 kJ) and the energy released upon forming the combustion products (CO_2 and H_2O: right), (blue bar: -4075.8 kJ).

Obligate, aero-tolerant and facultative anaerobes (such as *A. succinogenes*) are known to make use of fermentation and anaerobic respiration in anoxic environments. These systems are differentiated by the way they go about capturing energy. Whereas fermentation relies solely on substrate-level phosphorylation (SLP), in contrast anaerobic respiration utilises electron transport-coupled phosphorylation (ETP) for ATP synthesis, similar to the classic oxidative phosphorylation of aerobic respirations (Figure 2).

By this mechanism, the intermediate electron carriers NADH/NADPH are re-oxidised by specialised membrane-bound proteins, instead of merely disposing of the electrons (and their potential energy) into an endogenous electron acceptor.

These membrane-bound proteins constitute the initial phase of a larger organisation of similarly functioning proteins and molecules, which together embody an electron transport chain (ETC). As electrons are funnelled through sequential redox reactions of the ETC, the released energy from the shift in E_0' (i.e. $\Delta E_0'$) is subsequently used to translocate H^+ ions across a bi-lipid membrane against a concentration gradient before the electrons are deposited in a TeA (Willey et al., 2011).

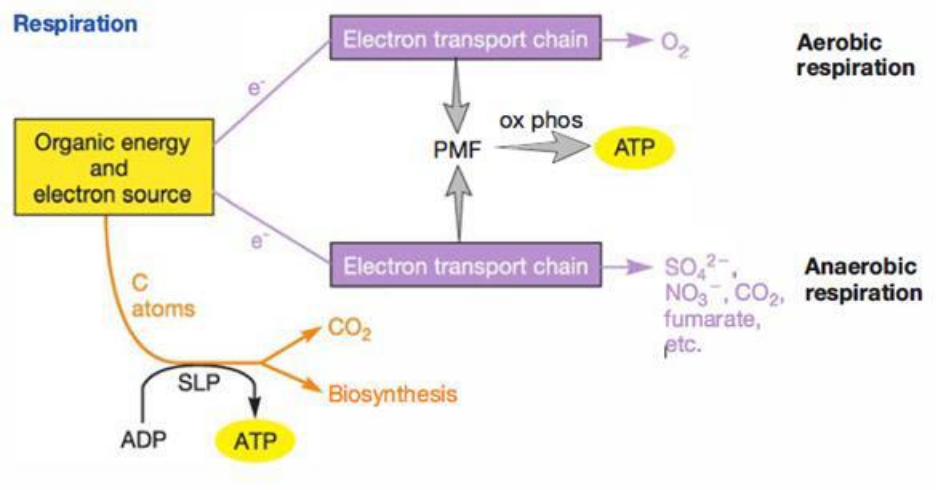

Figure 2: Summary of the energy acquisition mechanisms of both aerobic and anaerobic respiration.

Note: By utilising a PMF in addition to SLP for energy capture, anaerobic respiration pathways differ from fermentation which relies exclusively on SLP.

In this way catabolic reactions that yield less than the 44 $kJmol^{-1}$ required for ADP phosphorylation may become additive as a temporarily stored reservoir of potential energy, known as the proton motive force (PMF).

Depending on an organism's genetically available ETC pathways, one or more of several chemical entities may be used as a TeA. The particular TeA, as well as the specific ETC route used to conduct the electrons to it, denotes the degree of transmembrane H^+ concentration difference obtainable per mole substrate. In turn, this translates directly to the relative strength of the PMF and thereby the maximum ATP producible when H^+ ions re-enter the cytosol through the transmembrane protein H^+-dependent ATP synthase to drive ATP synthesis.

The chemiosmotic mechanism of respiration (first proposed by Mitchell, 1966) provides stoichiometric flexibility. By varying the total H^+/e^- ratio, a fractional APT yield is adjusted to the ΔG of the driving reaction. To this extent, more ATP can be produced per mole substrate since this form of ADP phosphorylation is not subject to the energy released by a single reaction.

2.1.1 Fumarate respiration

Among the many forms of anaerobic respiration (Myers & Kelly, 2005; Hadjipetrou & Stouthamer, 1965; Shi et al., 2007), fumarate respiration is unique. Unlike most other respiratory mechanisms, it utilises an endogenous carbon-based metabolite as its TeA (akin to that of fermentation). It is speculated to be the most widespread form of anaerobic respiration since fumarate can be readily synthesised from several organic carbon sources (Oren, 1991). This is due to the interlocking metabolic pathways already present in most organisms. Because of this, fumarate is generally freely available and therefore, theoretically, organisms need not rely on sourcing it from the environment as do other TeAs.

To date, various separate modes of fumarate respiration have been documented. Though similar in objective, the mechanisms employed and their associated energetics may differ considerably. By far the most thoroughly studied specimen of fumarate respiration is the microorganism *Wolinella succinogenes* (Kroger et al., 2002). As implied by its species name, this microbe is known to produce high titres of succinate.

Considering that the production of fumarate is endogenous, one would be inclined to think that succinate should be a fermentative end product. However, due to the enzyme responsible for succinate production being associated with the generation of a proton gradient, as has been shown in *E. coli*, it is, rather, an anaerobic respiration end product (Iverson et al., 1999; Lancaster, 2003). Furthermore, *W. succinogenes* has been shown to utilise several electron donors to facilitate fumarate reduction to enable growth (Kroger et al., 2002). These include dihydrogen, formate and sulphide (Reaction 1 a-c).

H_2 + fumarate → succinate (a)

HCO_2 + fumarate + H^+ → CO_2 + succinate (b)

HS^- + fumarate + H^+ → S + succinate (c) Reaction 1

In each case, the enzymatic complex is composed of two distinct membrane-bound components which are coupled to each other through a family of lipid-soluble intermediate electron carriers (Lemma et al., 1991). Depicted below is the molecular diagram that showcases the mechanistic aspects as described above by reactions *a* and *b* in Reaction 1 (Figure 3).

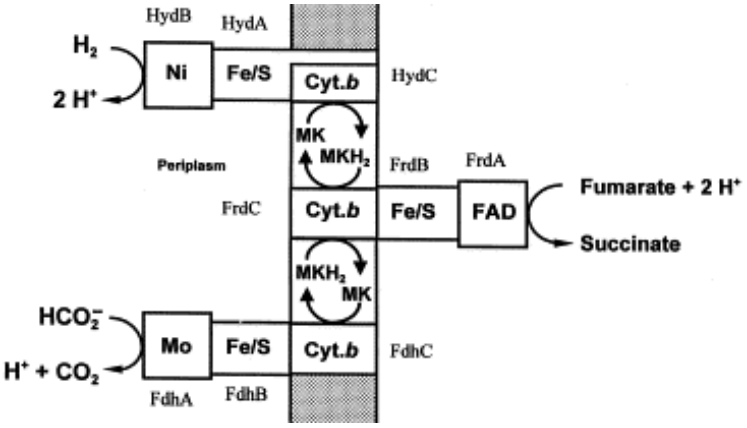

Figure 3: The electron transport system of *W. succinogenes* catalysing fumarate respiration with H_2 (Reaction 1 a) or formate (Reaction 1 b) (Kroger et al., 2002). Electrons are transferred by Hydrgenase (HydABC) from dihydrogen or Formate dehydrogenase (FdhABC) from formate to menaquinone (MK) to form menaquinol (MKH_2). Menaquinol then subsequently transfers the electrons to Formate reductase (FrdABC) witch deposits them in fumarate to produce succinate.

As can be seen from the image, an electron donor molecule is oxidised by a dehydrogenase. Electrons gained from this action are then used to reduce a quinone molecule. The then newly formed quinol is re-oxidised back to quinone by a fumarate reductase, which passes the electrons on to reduce fumarate to succinate.

During this process of cascading redox relay, protons are translocated across the membrane and, in this effort, energy is stored by way of a transmembrane proton concentration difference.

2.1.2 The H^+/ATP coupling mechanism

The chemiosmotic mechanism allows reactions that are insufficiently exergonic to drive SLP to still participate in ATP synthesis. The transmembrane proton gradient (Δp) generated by the components of the ETC acts as an energy reservoir, representing the sum of all its H^+ translocating driving reactions. ATP synthesis subsequently results when three H^+ ions pass through ATP synthase from the periplasm back into the cytoplasm (Brune et al., 1987). This process is called the proton motive force (PMF) and happens through passive but facilitated diffusion, similar to that of aerobic-associated ATP synthase found in numerous other organisms. In this regard, a single driving reaction may produce a 'fractional' yield of ATP due to it acting in consortium with the collective of parallel driving reactions.

Respiration, therefore, in short, can be described as the fixation of bio-active energy in the form of ATP at the expense of a transmembrane proton gradient. This key node in the respiratory energy production pathway is executed by a single universally conserved enzyme, ATP synthase. Experimental support of this enzyme's action in an artificial environment highlights its simple nature and relatively independent function (Brune et al., 1987). Apart from its mediated production, this enzyme has the capacity to operate largely unrestricted. Its productivity is subject mostly to biophysical parameters such as Δp and the availability of the ATP precursor molecules. Because of this ATP synthase's activity, as indispensable as it may be, it is completely reliant on upstream energy relay operations within the cell environment and by this mechanism its contribution to cellular energetics is tuned to aid in the pursuit of global homeostasis. Therefore, various coupling ratios are used when describing the energy dynamics of individual respiratory systems. These include the ATP/e^-, H^+/e^- and H^+/ATP ratios.

The three ratios mentioned are by no means fixed and may fluctuate between species. In addition, they may fluctuate to some extent within a single cell in accordance with environmental changes.

To elaborate, the H^+/ATP ratio refers to the stoichiometric relation between the number of protons re-entering the cell through ATP synthase to produce a single ATP molecule. Furthermore, the H^+/e^- ratio denotes the molar amount of H^+ ions translocated across the membrane per mole of electron shifted. Similarly, the ATP/e^- ratio designates the fractional

molar amount of ATP produced per e^- shifted. And although it seems natural to assume that the H^+/e^- and ATP/e^- ratios are linearly fixed to one another, considering that the H^+/ATP ratio is a constant within a cell, the opposite is true. Although the ATP/e^- ratio is dependent on H^+ translocating out of the cell, the PMF due to Δp does not necessarily pass through ATP synthase completely. Some microbes are known to use their PMF to fuel other ATP-independent processes, such as powering a flagellum (Koushik et al., 2008). In addition, ATP synthase activity is subject to the magnitude of Δp, meaning that a critical concentration would need to be surpassed to produce the diffusive pressure necessary for a stable ATP production (Bokranz et al., 1985).

2.2 Metabolic Pathways of *A. succinogenes*

Glycolysis of dextrose in *A. succinogenes* is known to occur via the Embden–Meyerhof–Parnas (EMP) pathway. This results in the production of 2 moles phosphoenolpyruvate (PEP) and 2 moles NADH for every mole dextrose consumed. At the PEP node, glycolysis couples to an incomplete tricarboxylic acid (TCA) cycle by branching into an oxidative C3 and a reductive C4 route.

When entering the oxidative C3 branch, PEP is converted into pyruvic acid (Pyr) by pyruvate kinase and consequently generates a single molecule of ATP by substrate-level phosphorylation (SLP). Pyruvate is then further catabolised to acetyl coenzyme A (AceCoA) by either pyruvate formate lyase (PFL) or pyruvate dehydrogenase (PDH). When conversion is by PFL, the production of AceCoA is accompanied by the liberation of a formic acid (For) molecule with no net production of NADH. Conversely, when conversion is by PDH, the production of AceCoA is accompanied by the release of a CO_2 molecule with the subsequent release of an NADH molecule. Furthermore, *A. succinogenes* retains the ability to convert formic acid into CO_2 through formate dehydrogenase (FDH) to release an NADH molecule. Therefore, the combinatory pathway of PFL and FDH has, in effect, the same resulting outcome as the PDH route. Next, AceCoA branches into fermentative production of either acetic acid (Ace) or ethanol (EtOH), the outcome of which is determined by the overarching cellular cofactor requirements. Effectively, AceCoA is converted to acetic acid by way of acetate kinase to

generate a mole of ATP through SLP, or it is converted to ethanol via acetaldehyde to spend 2 moles of NADH.

Alternatively, when channelled into the reductive C4 branch, PEP is carboxylated by phosphoenolpyruvate carboxykinase to produce an oxaloacetic acid (Oxa) and an ATP by way of SLP. From here on oxaloacetic acid is reduced to malic acid (Mal) by malate dehydrogenase, which is subsequently converted to fumaric acid (Fum) by fumarase. Finally, fumaric acid acts as a TeA and is reduced to succinic acid (Suc) by the membrane-bound enzyme fumarate dehydrogenase, operating as part of an electron transport chain (Figure 4, discussed in Section 2.1). This results in the generation of approximately 2/3 mol ATP for every mole of succinic acid produced (McKinlay et al. 2007).

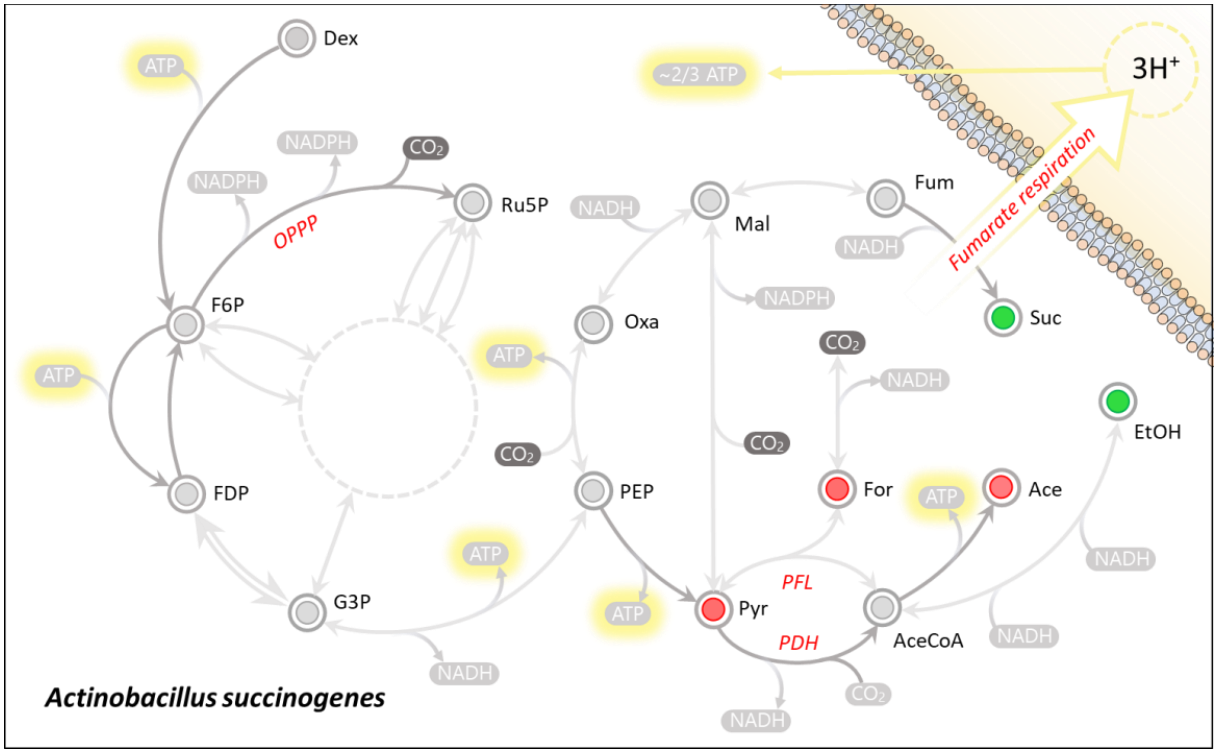

Figure 4: Main nodes of *Actinobacillus succinogenes* central carbon metabolism

Legend: Unidirectional arrows (dark) indicate proposed unidirectional fluxes (McKinlay et al., 2010), where all other fluxes are considered to be reversible. The dotted circle represents the pentose phosphate pathway overall reaction of the transketolase carbon exchange mechanism simplified to 3Ru5P ⇌ 2F6P + G3P. The red nodes (incl. For, Ace and Pyr) highlight metabolites that are net NADH-producing metabolites, whereas the green nodes (incl. Suc and EtOH) highlight net NADH-consuming metabolites.

Besides the PEP node, bridging links to the oxidative C3 branch are also found at Oxa and Mal, both of which couple to Pyr irreversibly and reversibly, respectively (Oxa bridge not shown in Figure 4). Both bridging links release the CO_2 captured in the initial phase of the reductive C4 branch. In addition, the malate bridge releases the reduction power gained during the conversion of oxaloacetic acid to malic acid, as NADPH. This provides *A. succinogenes* with a means to convert NADPH to NADH without employing transhydrogenase. This is effectively done by converting Pyr to Mal via the malate bridge, followed by oxidising Mal to Oxa and then returning to Pyr by either the oxaloacetate bridge or via PEP. This mechanism is only closed for the unidirectional conversion of NADPH to NADH. Reversing this process (i.e. NADH to NADPH) leads to an accumulation of pyruvic acid since both the oxaloacetate bridge and the conversion of PEP to Pyr are irreversible.

Branching off from the glucose-6-phosphate (G6P) node (not shown in Figure 4), the oxidative pentose phosphate pathway (OPPP) couples the hexose to the pentose metabolism and serves the purpose of generating reduction power by irreversibly splitting off a CO_2 and releasing two molecules of NADPH. Carbon entering the pentose metabolism from the OPPP is then rearranged by transketolase to rejoin the EMP pathway, with the net reaction that converts 3 mole ribulose-5-phosphate (Ru5P) to a mole of glyceraldehyde-3-phosphate (G3P) and 2 moles of fructose-6-phosphate (F6P).

Though it is not part of the central carbon metabolism, the carbon feeding into the abundant anabolic reactions of *A. succinogenes* diverges from 10 key nodes along its path (McKinlay *et al.,* 2007). These are: glucose-6-phosphate (G6P), fructose-6-phosphate (F6P), ribose-5-phosphate (R5P), erythrose-4-phosphate (E4P), glyceraldehyde-3-phosphate (G3P), 3-phosphoglycerate (3PG), phosphoenolpyruvate (PEP), pyruvate (Pyr), acetyl coenzyme A (AceCoA), and oxaloacetate (Oxa). Pathways, therefore, that feed toward these nodes are indispensable to the fundamental bio-operations of growth and cell division. For *A. succinogenes*, *de novo* production of biomass may be expressed as a summation of its constituents' origin along the central carbon metabolism as described by McKinlay (Reaction 2).

Biomass (1 g) = 410 µmol G6P + 126 µmol F6P + 686 µmol R5P + 244 µmol E4P
+ 99 µmol G3P + 1370 µmol 3PG + 528 µmol PEP + 2764 µmol Pyr
+ 3006 µmol AceCoA + 1502 µmol Oxa + 7813 µmol NH3
+ 13439 µmol NADPH – 2727 µmol NADH + 46930 µmol ATP Reaction 2

2.3 Energy Analysis

The flow of carbon flux through a metabolic system is driven by the intent to supply a ratio of specific metabolic precursors to anabolic branches, as directed by the given genome, as well as to fuel the energy demand of such *de novo* biomass production and its ensuing maintenance. Therefore, when regarding pure catabolism, the production of cellular waste products is associated with a stoichiometric amount of ATP generated through SLP and respiration. This provides a foundation for rationalising catabolite production dynamics as a function bio-available energy.

2.3.1 Main pathway assessment

Wild-type *A. succinogenes* is known to produce succinic, acetic and formic acid as its main catabolic products, with the occasional production of ethanol and pyruvic acid. Succinic acid production, as highlighted in Section 2.3, occurs via the reductive branch of the TCA cycle (Figure 4). This is due to the microbe lacking both a complete TCA cycle and a glyoxylate shunt, which would enable it to produce succinic acid oxidatively (McKinlay et al. 2007). By producing succinic acid in this way, *A. succinogenes* requires a molar equivalent of reducing power per mol succinic acid produced (Reaction 3).

$$1/2\ \mathrm{Dex} + \mathrm{CO_2} + \mathbf{NADH} \rightarrow \mathrm{Suc}\ (+\ 5/3\ \mathrm{ATP}) \qquad \text{Reaction 3}$$

To neutralise the redox imbalance caused by succinic acid production, the NADH deficit need be sourced from a complementary NADH-producing pathway. The organism

accomplishes this by diverting carbon flux from the Pyr node towards the oxidative production of acetic acid, in which case, pyruvate may be catabolised by either PFL or PDH (Reactions 4 & 5).

PFL: $1/2\ \mathrm{Dex} \rightarrow \mathrm{Ace} + \mathrm{For} + \mathbf{NADH}\ (+\ 2\ \mathrm{ATP})$ Reaction 4

PDH: $1/2\ \mathrm{Dex} \rightarrow \mathrm{Ace} + \mathrm{CO_2} + \mathbf{2\ NADH}\ (+\ 2\ \mathrm{ATP})$ Reaction 5

Although both pathways result in similar ATP yields, the PDH pathway produces twice the amount of reducing power compared with PFL. Therefore, to compare ATP production strategies between the two it is essential to consider the ATP production of the combinatory redox neutral route, normalised to a common base such as substrate consumed. With succinic acid production as the redox consuming branch and acetic acid production via PFL as the redox producing branch, the redox neutral energy pathway produces 11/3 mol ATP for every 6 Cmol dextrose consumed, an efficiency of 0.611 $mol_{ATP}Cmol_{Dex}^{-1}$ (Reactions 3 & 4; Figure 5).

By combining the two energy producing pathways in such a way as to achieve a redox neutral result, +5/3 ATP from the production of succinic acid, and +2 ATP from the production of formic and acetic acid is obtained. The sum of the total energy gained, +11/3 ATP, divided by the total C-moles substrate spent to obtain it (3 for succinic, 1 for formic, and 2 for acetic acid; 6 total), denotes the energy extraction efficiency of the redox neutral energy extraction pathway, 0.611 $mol_{ATP}Cmol_{Dex}^{-1}$.

Similarly, with the PDH-mediated acetic acid production route as the redox producing branch, an amount of 16/3 mol ATP is obtained for every 9 Cmol dextrose (6 for succinic, 2 for acetic, and 1 for CO_2), resulting in an efficiency of 0.593 $mol_{ATP}Cmol_{Dex}^{-1}$ (Reactions 3 & 5; Figure 5). By viewing ATP production as the objective of a redox neutral pathway, it becomes apparent that in terms of ATP yield per substrate consumed, the utilisation of the PFL and PDH routes does not result in the same energy extraction efficiency. The PDH pathway liberates slightly less energy – about 97% of that captured by PFL. Furthermore, FDH, which liberates NADH from formate in combination with the PFL route, results in an ATP capture efficiency identical to that of the PDH route.

Besides acetic and formic acid production, *A. succinogenes* has also been reported to secrete pyruvic acid, a net redox producing metabolite (Reaction 6).

$$1/2\ \text{Dex} \rightarrow \text{Pyr} + \mathbf{NADH}\ (+\ \text{ATP}) \qquad \text{Reaction 6}$$

When pyruvic acid production is substituted as the redox producing complement, an amount of 8/3 mol ATP is obtained per 6 Cmol dextrose (0.444 $mol_{ATP}Cmol_{Dex}^{-1}$) (Reactions 3 & 6; Figure 5). This approximates to 73% of the energy that could have been captured if the PFL route had been followed through, and therefore puts it in a less desirable position to produce, in terms of maximising energy capture.

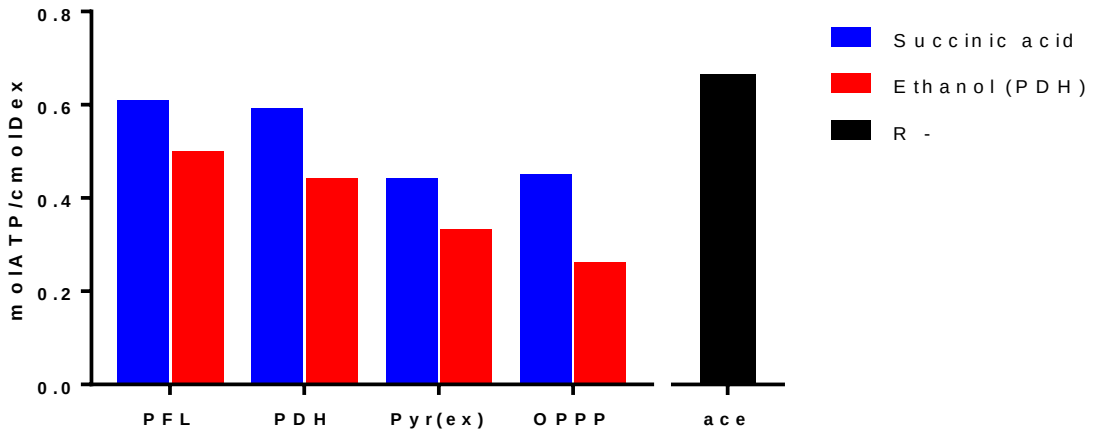

Figure 5: Visual comparison of static energy extraction efficiencies of PFL, PDH, pyruvate excretion and OPPP of *A. succinogenes*.

Legend: Energy extraction efficiency (y-axis) of redox producing pathways (x-axis) when coupled to succinic acid as redox consuming counterpart (blue) or ethanol as redox consuming counterpart (red). R-: energy extraction efficiency when reducing power is lost to the environment, producing only an acetic acid, shown in black.

Furthermore, a study done by Bradfield & Nicol (2016) has also made a case for the OPPP as a viable redox producing complement (Reaction 7).

$$1/6\ \mathrm{Dex} \rightarrow \mathrm{CO2} + \mathbf{2\ NADPH}\ (-\ 1/6\ \mathrm{ATP}) \qquad \text{Reaction 7}$$

Here too, due to the energy-consuming nature of the OPPP, the ATP gained per consumed substrate is significantly lower when compared with either of the acetic acid production strategies, yielding only 19/6 mol ATP gained per 7 Cmol dextrose consumed (0.452 $mol_{ATP}Cmol_{Dex}^{-1}$) (Reactions 3 & 7; Figure 5), roughly 74% of that produced by the PFL as the redox producing complement.

2.3.2 On ethanol production

In addition to succinic acid, *A. succinogenes* also maintains the ability to produce ethanol as a net redox consuming product when produced by the aid of the PFL route (Reaction 8).

$$1/2\ \mathrm{Dex} + \mathbf{NADH} \rightarrow \mathrm{EtOH} + \mathrm{For}\ (+\ \mathrm{ATP}) \qquad \text{Reaction 8}$$

A glance at the pathway's energy limitations highlights why succinic acid is favoured above ethanol production. When combined with PFL-aided acetic acid production as the redox producing complement (Reaction 4), an efficiency of 0.500 $mol_{ATP}Cmol_{Dex}^{-1}$ is obtained (Reactions 4 & 8; Figure 5). This covers only 82% of the energy that would have been gained with succinic acid production as the redox consuming branch. Likewise, the PDH-aided acetic acid production, pyruvate excretion and OPPP redox producing routes, coupled with ethanol production as the redox consuming complement, respectively result in 75% (0.444 $mol_{ATP}Cmol_{Dex}^{-1}$) (Reactions 5 & 8; Figure 5), 75% (0.333 $mol_{ATP}Cmol_{Dex}^{-1}$) (Reactions 6& 8; Figure 5), and 58% (0.262 $mol_{ATP}Cmol_{Dex}^{-1}$) (Reactions 7& 8; Figure 5) of the energy that would have been gained if succinic acid had been the redox consuming complement.

Ethanol may also be produced as a redox neutral product when produced via the PDH route (Reaction 9). This method, too, results in a low ATP production efficiency (0.333 $mol_{ATP}Cmol_{Dex}^{-1}$).

$1/2\ \mathrm{Dex} \rightarrow \mathrm{EtOH} + \mathrm{CO_2}\ (+\ \mathrm{ATP})$ Reaction 9

Although various studies have reported some ethanol accumulation, these efficiencies emphasise why its production is low or lacking, as at best it supplies only 82% of the energy supplied by succinic acid. It is, therefore, the author's opinion that the organism retains the ability to produce ethanol primarily as a failsafe to an obstruction of succinic acid production, such as when CO_2 mass transfer is insufficient, to rid itself of toxic redox build-up (Herselman et al., 2017). Furthermore, it may serve to support succinic acid production in such instances by recycling the CO_2 generated by ethanol production to obtain better ATP production efficiencies. These efficiencies, when considering no net production or consumption of CO_2, range from 0.346 to 0.528$mol_{ATP}Cmol_{Dex}^{-1}$,the highest being obtained when ethanol is produced via the PDH pathway as a redox neutral product to supply a CO_2 molecule towards succinic acid production coupled to the PFL- or PDH-mediated acetic acid production.

2.3.3 Other theoretical pathways

Although no studies report their accumulation, *A. succingenes* actively manufactures the dicarboxylic acids: oxaloacetic, malic and fumaric acid. Therefore, if one is to reconcile production behaviour to ATP gain, a closer look at all energy production pathway efficiencies is warranted.

Both malic and fumaric acid are produced as redox neutral products, with the liberation of a single molecule of ATP (Reactions 10 & 11).

$1/2\ \mathrm{Dex} + \mathrm{CO_2} \rightarrow \mathrm{Mal}\ (+\ \mathrm{ATP})$ Reaction 10

$1/2\ \mathrm{Dex} + \mathrm{CO_2} \rightarrow \mathrm{Fum} (+\ \mathrm{ATP})$ Reaction 11

This puts them in the same league as ethanol production as a redox neutral product in terms of energy production efficiency, each gaining just 0.333 $mol_{ATP}Cmol_{Dex}^{-1}$. This indicates

that their eventual excretion would be just as unlikely, if not even more unlikely, as the redox neutral production of ethanol. Contrary to ethanol, the production of oxaloacetic and malic acid requires the incorporation of a CO_2 molecule and therefore there is no incentive for their production. The absence of these acids provides support for the notion that ethanol production only acts as a failsafe for the microbe in an environment starved of CO_2.

Oxaloacetic acid, similar to pyruvic acid, produces a single molecule of NADH and ATP. In addition, its production requires the incorporation of a CO_2 molecule (Reaction 12).

$$1/2\ \mathrm{Dex} + \mathrm{CO2} \rightarrow \mathrm{Oxa} + \mathbf{NADH}\ (+\ \mathrm{ATP}) \qquad \text{Reaction 12}$$

Participating as a redox production complement, coupled to succinic acid production, oxaloacetic acid delivers an ATP production efficiency of 0.444 $mol_{ATP}Cmol_{Dex}^{-1}$ (Reactions 3 & 12). This efficiency is similar to that obtained from pyruvic acid production. Since oxaloacetic acid production in *A. succinogenes* is not reported in the literature, this signifies some controversy as to the production of pyruvic acid which, in contrast, is indeed reported in the literature. This matter is further explored in Section 4.4.

2.3.4 External redox loss or gain

Interestingly, when supplied with a free external source of redox, homosuccinic acid production will occur at 0.556 $mol_{ATP}Cmol_{Dex}^{-1}$, which still is less energy than would have been gained if acetic acid production had been in effect. However, in such a scenario where an abundance of external redox is supplied, an energy optimisation strategy should default to homosuccinic acid production, because any catabolite production associated with NADH liberation will be inaccessible.

Alternatively, in a scenario in which redox is lost to an external source, homoacetic acid production is likely to occur at an efficiency of 0.667 $mol_{ATP}Cmol_{Dex}^{-1}$, the highest achievable energy production efficiency of *A. succinogenes*. This efficiency, however, is normally inaccessible to the microbe due to closed-system redox balancing constraints.

3 Experimental

3.1 Materials

3.1.1 Microorganism

A. succinogenes 130Z (DSMZ 22257; ATCC 55618), procured from the German Collection of Microorganisms and Cell Culture (DSMZ), was propagated in 100 mL of Tryptic soy broth (TSB) at 37 °C to an OD_{660} of 1.0, at which time the culture was cryogenically preserved (-40 °C) in 2 mL cryotube containers by suspending 0.5 mL of culture broth in 1 mL of sterile glycerol. This procedure was done to ensure genetic stability throughout experimentation. Before experimental start-up cells were revived from cryostasis by allowing the stock to thaw to ambient temperature and subsequently aseptically inoculating it into 25 mL screwcap vials containing 20 mL of sterile TSB, pre-heated to 37 °C. These starter cultures were then incubated for 16–24 h at 37 °C and 250 rpm, after which 10 mL of the volume was aseptically transferred to the bioreactor via a hypodermic needle.

3.1.2 Feed materials

All chemicals were of reagent grade and purchased from Sigma-Aldrich (St. Louis, Missouri, USA), except for dextrose monohydrate, which was purchased from Bragan Chemicals (Johannesburg, South Africa), and CO_2 (g), obtained from Afrox (Johannesburg, South Africa). In this study, two separate media compositions were used.

The final composition of growth medium A consisted of: 50.0 gL^{-1} dextrose, 10.0 gL^{-1} clarified corn steep liquor (CSL), 6.0 gL^{-1} yeast extract (YE), 0.2 gL^{-1} $MgCl_2.6H_2O$, 0.2 gL^{-1} $CaCl_2.2H_2O$, 1.0 gL^{-1} NaCl, 3.0 gL^{-1} K_2HPO_4, 1.6 gL^{-1} NaH_2PO_4, and 0.31 gL^{-1} Na_2HPO_4. Clarified corn steep liquor was prepared by heating a 200 gL^{-1} solution to 105 °C for 15 min and then decanting the supernatant once all solids had precipitated after cooling. Dextrose and phosphates were autoclaved separately from other media components (121 °C for 60 min), with the mixtures being aseptically combined once they had cooled down to ambient temperature. This was done to prevent unwanted reactions occurring. Glucopyranose, a cyclic hemiacetal, in equilibrium with its open-chain aldehyde sugar structure dextrose, an aldohexose, will bond readily to proximate amines. Many of these reactions are irreversible and their products are inaccessible to bacteria (Black, 1997). Furthermore, all phosphates, apart from those of sodium, potassium and ammonium, are insoluble. Therefore, most ion exchange reactions would result in the precipitation of the phosphates out of solution, negating their effect as effective buffering agents.

Similarly, growth medium B consisted of (final composition): 50.0 gL^{-1} dextrose, 1.7 gL^{-1} yeast nitrogen base without amino acids (YNB), 0.3 gL^{-1} yeast extract (YE), 3.0 gL^{-1} Tryptic soy broth (TSB), 3.0 gL^{-1} K_2HPO_4, 1.6 gL^{-1} NaH_2PO_4, 0.31 gL^{-1} Na_2HPO_4, 1.0 gL^{-1} NaCl, 2.0 gL^{-1} NH_4Cl, 10 mgL^{-1} biotin, 25 mgL^{-1} nicotinamide, 150 mgL^{-1} glutamic acid, 80 mgL^{-1} methionine, and 80 mgL^{-1} cysteine (based on McKinlay et al., 2005). Components that could not be subjected to the extreme temperatures of the autoclaving procedure were added to the autoclaved mixture by filtration using a 0.2 µm liquid filter (Midisart 2000, Sartorius, Göttingen, Germany).

3.1.3 Fermentation setup

The fermenter of choice consisted of a 2.0 L reservoir jacketed-reactor vessel (1.5 L working volume), to which were coupled external high-flow liquid and gas peristaltic recycle lines (Figure 6). Both recycle lines were made of inert silicone tubing and served to agitate the liquid bulk to a homogeneous composition. Furthermore, the liquid recycle line acted as a port for (i) an in-line aluminium pH/temperature probe station housing a Tophit CPS417D glass probe (Endress+Hauser, Gerlingen, Germany), (ii) a 10 M NaOH dosing inlet, (iii) an aseptic CO_2 gas inlet, (iv) a sample outlet, and (v) a low liquid flow recycled bleed stream (at ca 100 mL/min) incorporated with an in-line spectrophotometric flow cell. Excessive foaming was controlled by dripping a 10% (v/v) Antifoam SE-15 solution onto the bulk liquid surface when needed. In addition, the vessel contained a septum sealed inoculation port, a 0.2 µm PTFE filter fitted gas outlet port (Midisart 2000, Sartorius, Göttingen, Germany) to maintain atmospheric pressure, and a medium inlet port which was used to fill the vessel prior to experimental start-up. Gas flow was controlled with a Brooks Mass Flow Controller (Hatfield, PA, USA), and CO_2 was fed at a constant 30% vvm to saturate the medium and displace all dissolved O_2. Heated water was continuously circulated to the heating jacket from a separate 5.0 L stirred vessel (4.0 L working volume) which was in direct contact with a custom PID-controlled heating plate. Fermentation was controlled at 37 °C (± 0.6) and a pH of 6.8 (± 0.05) utilising a Liquiline CM442 (Endress+Hauser, Gerlingen, Germany), coupled to a custom-developed LabVIEW 2017 program (National Instruments), which toggled the output of the heating plate and peristaltic NaOH dosing pump on/off using a relay.

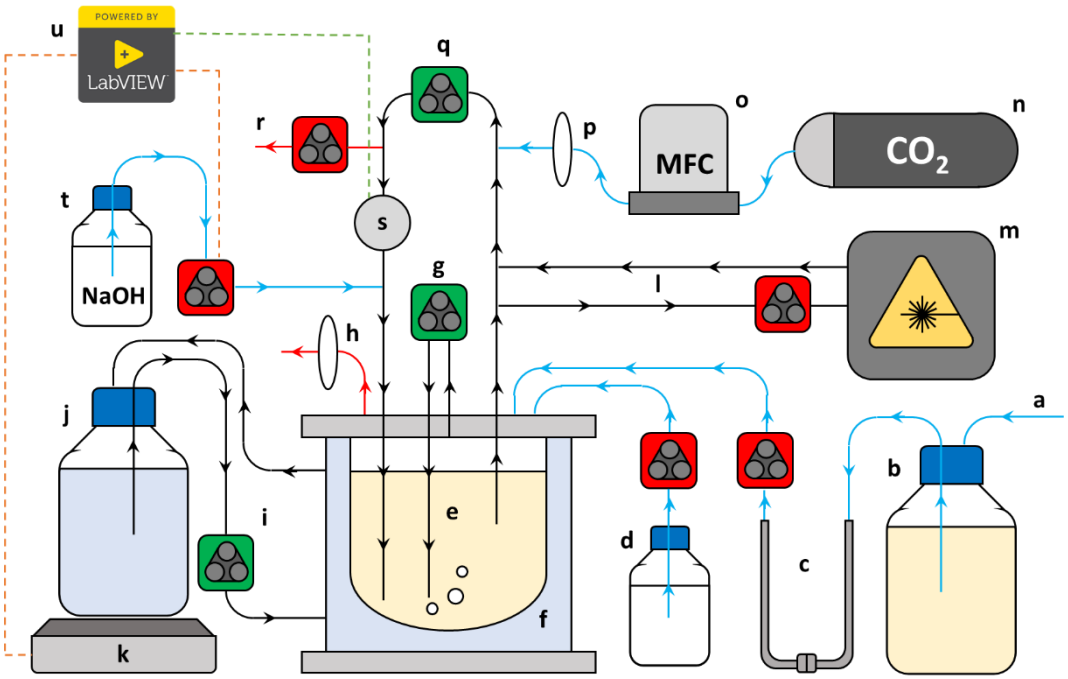

Allocation	Description
a	multiple sterile inlet lines
b	medium reservoir
c	detachable U-connection (sterilised in oil bath)
d	antifoam reservoir
e	reactor vessel
f	water jacket
g	gas recycle line
h	gas outlet
i	heat transfer recycle line
j	heated water reservoir
k	hotplate
l	spectrophotometer recycle line
m	flow cell spectrophotometer
n	CO_2 gas tank
o	mass flow controller
p	air filter
q	liquid recycle line
r	sample line
s	temperature/pH probe
t	NaOH reservoir
u	LabVIEW™-operated temperature/pH controller coupled to the input (s, green stippled line) to subsequently regulate the outputs (t & k, red stippled lines)

* Pumps: high velocity (green), low velocity (red).
* Recycle lines (black), inlet lines (blue), outlet lines (red).

Figure 6: Fermentation setup – Simplified scheme of reactor setup

3.2 Experimental Operation

3.2.1 Fermentation start-up

Before start-up, the entire system (excluding the NaOH) was autoclaved at 121 °C for 60 min, after which the reactor and sterilised feed were aseptically coupled through a custom-made stainless-steel U-connector which was then sterilised by immersion in an oil bath (140 °C for 30 min). Subsequently, when the system had cooled to ambient temperature, the medium was transferred to the reactor and sparged with CO_2 for 1 h at a rate of 30 vvm. Following the initial sparging step, dosing was switched on and the reactor was allowed to come up to the fermentation temperature while still continually sparging.

Once the reactor had stabilised at the desired pH and temperature (pH 6.8, 37 °C), the reactor was allowed to run for 16–24 h while the inoculum was cultivating, during which time the OD_{660} absorption was monitored for the presence of contamination. With HPLC confirmation of a sterile environment, 10 mL inoculum was aseptically transferred to the reactor via a hypodermic needle. After allowing for a one-minute mixing time, the OD_{660} baseline was zeroed and a t_0 sample was taken.

3.2.2 Sampling method

Over the experimental timespan (70–100 h), 20 to 30 x 2 mL samples were collected, including the one at start-up (t_0). Due to the dead volume of the outlet line, the line was flushed by discarding the first 2 mL collected before sample acquisition. Samples were then immediately placed on ice to halt metabolic activity and the time of acquisition recorded. Thereafter they were immediately centrifuged on a benchtop centrifuge (at 13 000 rpm for 90 s at room temperature) and passed through a 0.45 µm filter to remove cellular biomass, and the composition of each sample was then determined in triplicate by HPLC analysis. Samples that could not be analysed directly were stored at -80 °C to prevent physical degradation and microbial growth.

3.3 Analytical Methods

3.3.1 HPLC analysis

Sample composition was determined by HPLC analysis, using an Agilent 1260 Infinity HPLC system (Agilent Technologies, USA) equipped with a 300 x 7.8 mm Aminex HPX-87H ion-exchange column (Bio-Rad Laboratories, USA) and a refractive index detector.

Both a 0.3 mL L^{-1} and a 1.5 mL L^{-1} H_2SO_4 mobile phase were used for sample analysis. This was done due to the co-elution of peaks and allowed the accurate measurement of all compounds of interest. In both cases, the measurement was conducted at a flow rate of 0.6 mL min^{-1} and a column temperature of 60 °C. The samples were analysed in triplicate for each mobile phase condition and screened for the abundance of phosphates, dextrose, ethanol, glycerol, and for citric, oxaloacetic, malic, fumaric, succinic, pyruvic, acetic and formic acid. Moreover, lactic acid concentration was monitored and its accumulation was used as a benchmark for infection, in which case the fermentation was immediately terminated.

The phosphates peak was used as an internal standard since its profile remains constant throughout fermentation, and therefore all other measured metabolite concentrations were adjusted accordingly to factor out the effect of dilution errors resulting from NaOH dosing and antifoam addition.

3.3.2 Biomass quantification

Suspended dry cell weight (DCW) accumulation was measured online using an Agilent Cary 60 UV-Vis Spectrophotometer (Agilent Technologies, USA) equipped with a Quartz Micro Flow Cell (10 mm path length; 70 µL internal volume) connected in-line to the secondary liquid recycle line of the fermenter. High-resolution growth profiles were obtained by collecting a 1 s averaged absorbance measured at OD_{660} every 4.8 s. Absorbance values were then converted to concentrations based on a function fitted to a standard curve determined for the DCW of *A. succinogenes*.

Samples used for setting up the DCW-OD_{660} correlation were centrifuged at 13 000 rpm for 90 s, after which the cell pellets were washed twice with PBS solution and the cellular biomass was suspended and re-centrifuged, and then dried for 48 h at 85 °C.

3.4 Data Analysis

Curve fitting, manipulation and analysis of the data were done with the aid of GraphPad Prism 7.00 software (GraphPad Software, USA). The data was used to fit either a four-parameter or biphasic logistic equation for each of the compound profiles, with the bottom parameter constrained to zero.

Best fit curves were subsequently used for further rate-based analysis. Due to *A. succinogenes* having an inherent nature to produce biofilm, spectrophotometric determination of biomass accumulation only proved useful until such time that flocculation occurred. Thus, DCW measurements of the final biomass concentration were measured in triplicate and corrected for volume changes due to NaOH and antifoam addition. This measurement served as an upper limit constraint when fitting the logistic growth curves.

Rate-based mass and redox balances were performed to assess the closure and accuracy of metabolite measurement. Mass balances were performed by calculating the stoichiometric amount of dextrose needed to satisfy the production of biomass and the catabolites measured, and by comparing this against the change in the measured amount of dextrose (Villadsen et al., 2011). Similarly, redox balances were performed by calculating from the measured catabolites the stoichiometric amounts of redox produced and consumed. These balances serve as a tool to assess absolute metabolic activity by indicating whether all mass and charge have been accounted for. Discrepancies in the closure of these balances are indicative of unaccounted-for metabolic processes.

4 Results and Discussion

4.1 Batch Fermentation Data Acquisition

The acid concentration data obtained were fitted with asymmetrical (five-parameter) or bi-logistic curves, depending on their goodness of fit. Fitting of the data was done with the aid of GraphPad Prism software. With their bottom parameter constrained to zero, the curves generally presented with an R^2 parameter >0.99. However, curves were deemed representative of the data at values greater than 0.95 (Figure 7 and Table 1).

The concentration profiles generated by both media compositions displayed comparable trends with repeat batches and were therefore considered to be representative of the particular conditions at which they were tested.

With regard to the biomass quantification, both media tested repeatably displayed the initial phases of logistic growth, followed by an extensive and erratic reduction in the measured concentration. This occurred at the onset of flocculation (a brief period in which the measured concentration became less stable but still maintained an increasing slope) and

eventual biofilm deposition, resulting in a reduction of biomass measured by spectrophotometry (Figure 7).

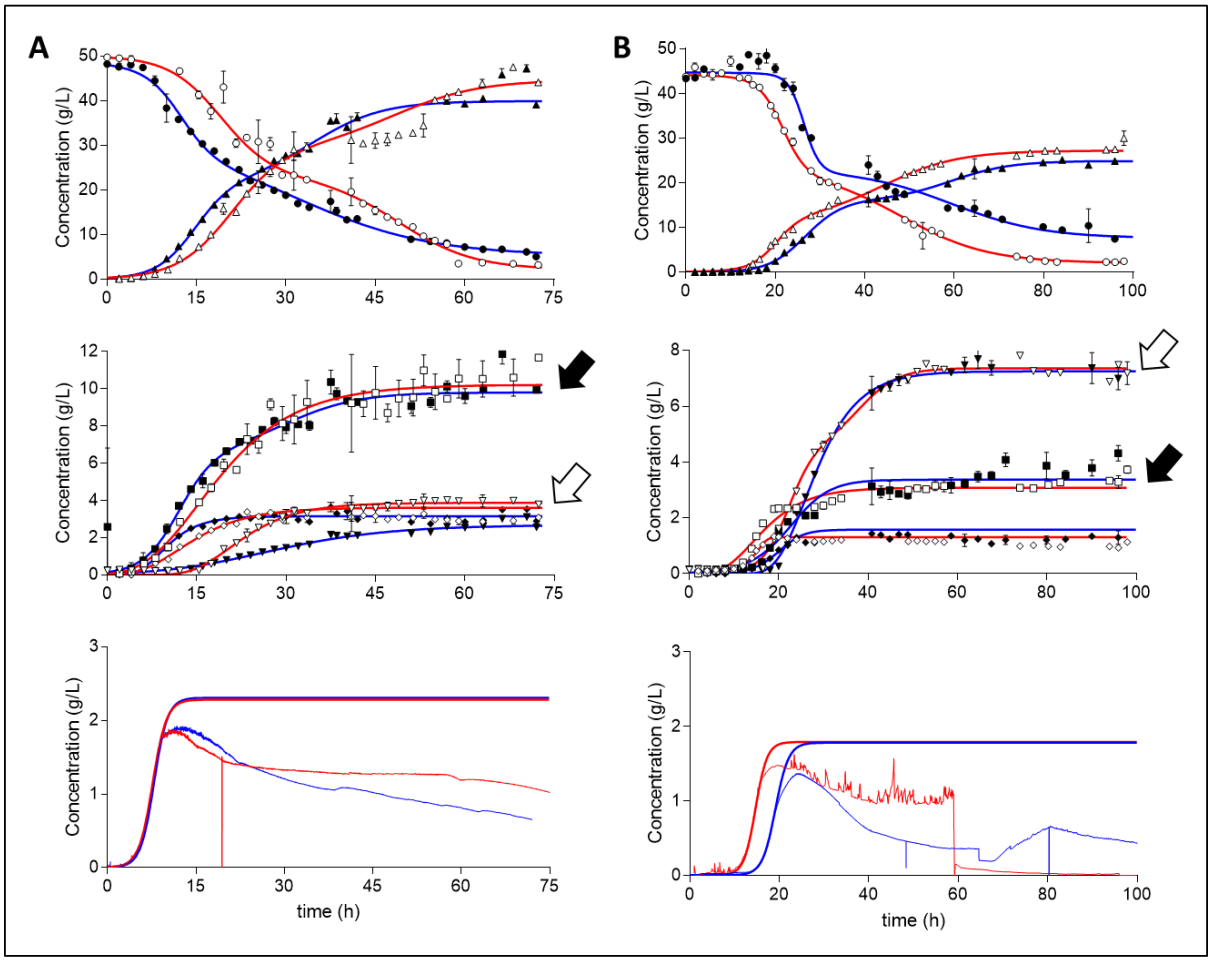

Figure 7: Repeat batch concentration profiles (gL^{-1}) of *A. succinogenes* on medium A and medium B

Legend: Dextrose, ○; succinic acid, △; acetic acid, □; formic acid, ◇; pyruvic acid▽; repeats are indicated as filled shapes with blue fits. Biomass profiles (bottom) display online OD_{660} absorbance data and their logistic fits, with the top parameter fixed to a final DCW-determined concentration. Black arrows (acetic acid) and white arrows (pyruvic acid) highlight the shift in their relative abundance between the two media.

To acquire the entire profile, the precipitated biofilm was resuspended and homogenised in the liquid broth after the experimental runs, after which measurements of DCW were made in triplicate to fix the final biomass concentration. To the end point (as measured by DCW) and to the high-resolution data of the initial stages of platonic growth, a four-parameter logistic curve was fitted to gain an accurate representation of the biomass accumulation during the batch fermentative lifespan of *A. succinogenes.*

As can be observed in Figure 7, clear repeatable logistic curves were obtained for medium A and repeatable, but time-delayed, curves were evident in medium B. Repeat batches resulted in similar DCW endpoints. It is likely that a lower initial starting concentration of viable cells in the inoculum caused the ~4 h time-delay shift seen in one of the batch fermentations of medium B.

It is evident from the data that medium A consistently displayed a higher accumulation of succinic, acetic and formic acid compared with medium B (Table 1). Another key difference observed was the amount of measured pyruvic acid. Interestingly, medium B resulted in the excretion of nearly twice the amount of pyruvic acid compared with medium A. Secondly, pyruvic acid was found to be the second most abundant acid present in medium B after succinic acid. This is indicative of a probable bottleneck effect. Unlike the standard response generated by medium A, it is evident that the oxidative step from pyruvic to acetic acid was significantly suppressed. In either medium A and medium B no measurable accumulation of ethanol or of oxaloacetic, malic, fumaric or lactic acid was evident.

Table 1: Goodness of fit (R^2) of each fitted curve and their respective titres (gL^{-1}) at fermentation termination

		A - 1	**A - 2**	**B - 1**	**B - 2**
Succinic acid	g L^{-1}	44.62	39.89	27.20	24.87
	R^2	*0.9978*	*0.9984*	*0.9987*	*0.9977*
Pyruvic acid	g L^{-1}	3.870	2.766	7.363	7.252
	R^2	*0.9863*	*0.9886*	*0.9980*	*0.9958*
Acetic acid	g L^{-1}	10.22	9.802	3.081	3.369
	R^2	*0.9645*	*0.9935*	*0.9737*	*0.9590*
Formic acid	g L^{-1}	3.604	3.145	1.312	1.577
	R^2	*0.9937*	*0.9985*	*0.9933*	*0.9945*
Biomass	gL^{-1}	3.272	3.300	2.640	2.700
	R^2	*0.9995*	*0.9976*	*0.9848*	*0.9888*
Dextrose	gL^{-1}	2.172	5.293	2.047	7.581
	R^2	*0.9949*	*0.9991*	*0.9996*	*0.9866*

Of note is that the pyruvic acid excretion rates and the final pyruvic acid concentration reached for the two batch runs in medium A were found to be significantly different. The repeat run displayed less of a rapid accumulation profile.

Further analysis of this data highlights run 1 of medium A and run 2 of medium B as these runs had accompanying measured ORP data.

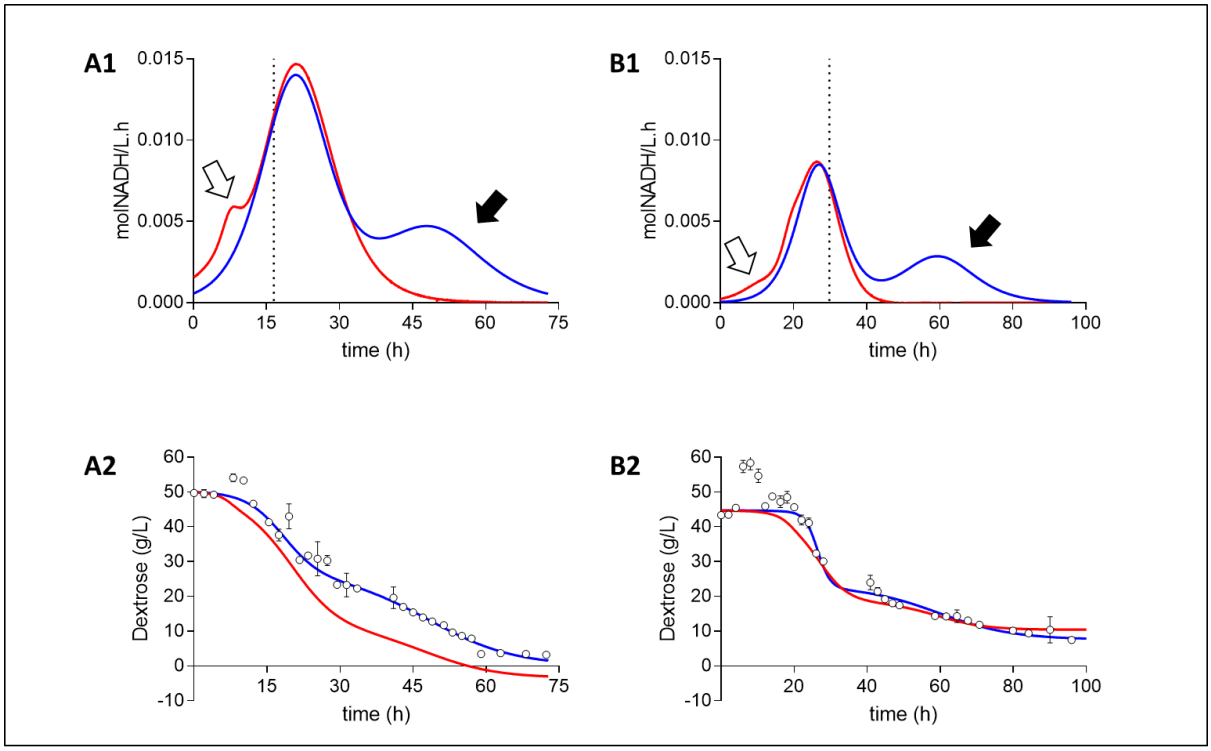

Figure 8: Fermentation redox and mass balances of medium A and medium B

Legend: Redox balances (A1, B1): Volumetric NADH consumption rate (blue) and production rate (red) as calculated from the measured catabolites (Suc, Pyr, Ace, For). White arrows show the net NADH production with no measured consuming counterpart, while black arrows show the net measured redox production with no measured redox producing counterpart. The dotted lines signify the termination of growth. Mass balances (A2, B2): Measured dextrose concentration (circles) and their fits (blue) are compared to the predicted dextrose concentration (red) as determined from the measured metabolite concentrations. A near-accurate closure is obtained in medium B while medium A continuously displays lower dextrose consumption than is predicted, attributed to the additional carbohydrate content of CSL and YE.

4.2 Redox Balances

Redox balances displayed a similar trend across both media compositions (Figure 8). Volumetric rate analysis revealed a scenario in which redox was being produced at a faster rate than it was consumed during the initial stages of growth, as indicated in the derived production and consumption rate profiles of Figure 8. This was followed by a regime of near-to-complete redox closure, and then by a phase in which more redox was being consumed than could be accounted for alone by the redox producing metabolites measured.

The initial stages of higher redox production rates coincided with a drop in the medias oxidoreduction potential (ORP). A rapid shift to approximately −370 mV occurred during the initial stages of growth, after which the measurement stabilised (Figure 9). A similar observation has been reported in the literature (Li et al., 2010). In contrast, the final stages of the fermentation displayed overconsumption of redox (based on measured metabolites), providing a clear indication of an unmeasured redox producing metabolite.

Here it is thought that the OPPP is the likely culprit as the pathway results in no additional catabolites other than CO_2 (Bradfield & Nicol, 2016). Since the production of succinic acid entails the incorporation of CO_2, the reactor was sparged with CO_2 to saturate the environment. For this reason, gas analysis was not performed to verify OPPP activity. However, since no additional catabolites were measured in the liquid phase, the OPPP seems the most likely explanation. This suggests a state of homo-succinic acid production towards the end of batch fermentation.

4.3 Mass Balances

Mass balances were performed on the fitted graphs to establish whether mass closure could provide supporting evidence favouring OPPP activity by assuming that the unmeasured redox production came from the OPPP.

This was performed by comparing the dextrose consumption measured to the theoretical dextrose consumed. The theoretical dextrose consumed was calculated from the sum of the C-mole portion of each catabolite measured which originated from the dextrose substrate, and assuming an alpha value of 0.1 *[alpha value refers to the Cmol fraction of CO_2 generated for every Cmol de novo biomass produced]* (Equation 1).

$$\text{Dex (CmolL}^{-1}\text{)} = 3/2\ \text{Ace (CmolL}^{-1}\text{)} + \text{Pyr (CmolL}^{-1}\text{)} + 3/4\ \text{Suc (CmolL}^{-1}\text{)} + 1.1\ \text{Bio (CmolL}^{-1}\text{)}$$

Equation 1

Medium B exhibited a near-to-complete carbon closure, whereas medium A presented with more Cmol metabolites produced than Cmol dextrose consumed. This

deviation, however, is small enough for the carbon gain to be explained by the additional source of carbohydrate and amino acid compounds present in the 10 g L^{-1} CSL and 6 g L^{-1} YE, in addition to the dextrose in medium A. Although mass balance closure could not be demonstrated in medium A, the near closure in medium B suggests that the observed redox imbalance towards the end of fermentation is very probably the cause of unmeasured OPPP flux activity and not an unmeasured catabolite. The reasoning for this is that should an unmeasured net NADH producing catabolite have been the complement to the redox imbalance observed, the mass balance would have predicted less dextrose consumed than was measured.

It should be noted that the theoretical calculated dextrose consumed does not include the contribution of CO_2 lost by OPPP flux. However, this only means that the theoretical glucose consumed is slightly underestimated, making it even less likely that an unmeasured catabolite could have been the complement to the apparent excess redox consumed measured.

4.4 Linking Energy Acquisition and the Observed Metabolic Shift

Batch fermentation on *A. succinogenes* typically yields a shifting product distribution profile as fermentation progresses. Furthermore, it was previously reported by this research group that the product distribution profiles changed with increasing dextrose consumption when measured in a continuous bioreactor (Bradfield & Nicol, 2014). These researchers reported that the concentration of succinic acid increased with an increasing dextrose consumption, whereas concentrations of acetic and formic acid both increased initially and then subsequently flattened out or steadily decreased to zero, respectively. For this to occur, changes in metabolic strategies take place in which one enzymatic route is newly favoured over another to achieve a state of homeostasis.

One possibility considered is that these changes are the result of an energy optimisation mechanism exploited by the organism to thrive in an increasingly harsh environment. Although the simple theoretical analysis, as discussed in Section 2.3, supports this idea and

provides a reason as to why *A. succinogenes* fermentations start with a near-stellar 1:1:1 ratio production of succinic, acetic and formic acid – from an energy efficiency perspective – it does not offer clarity on why the metabolic shift would occur. To expand on this idea, the high-resolution batch fermentation profiles were generated to determine whether a consistent chronology could be found (Figure 7).

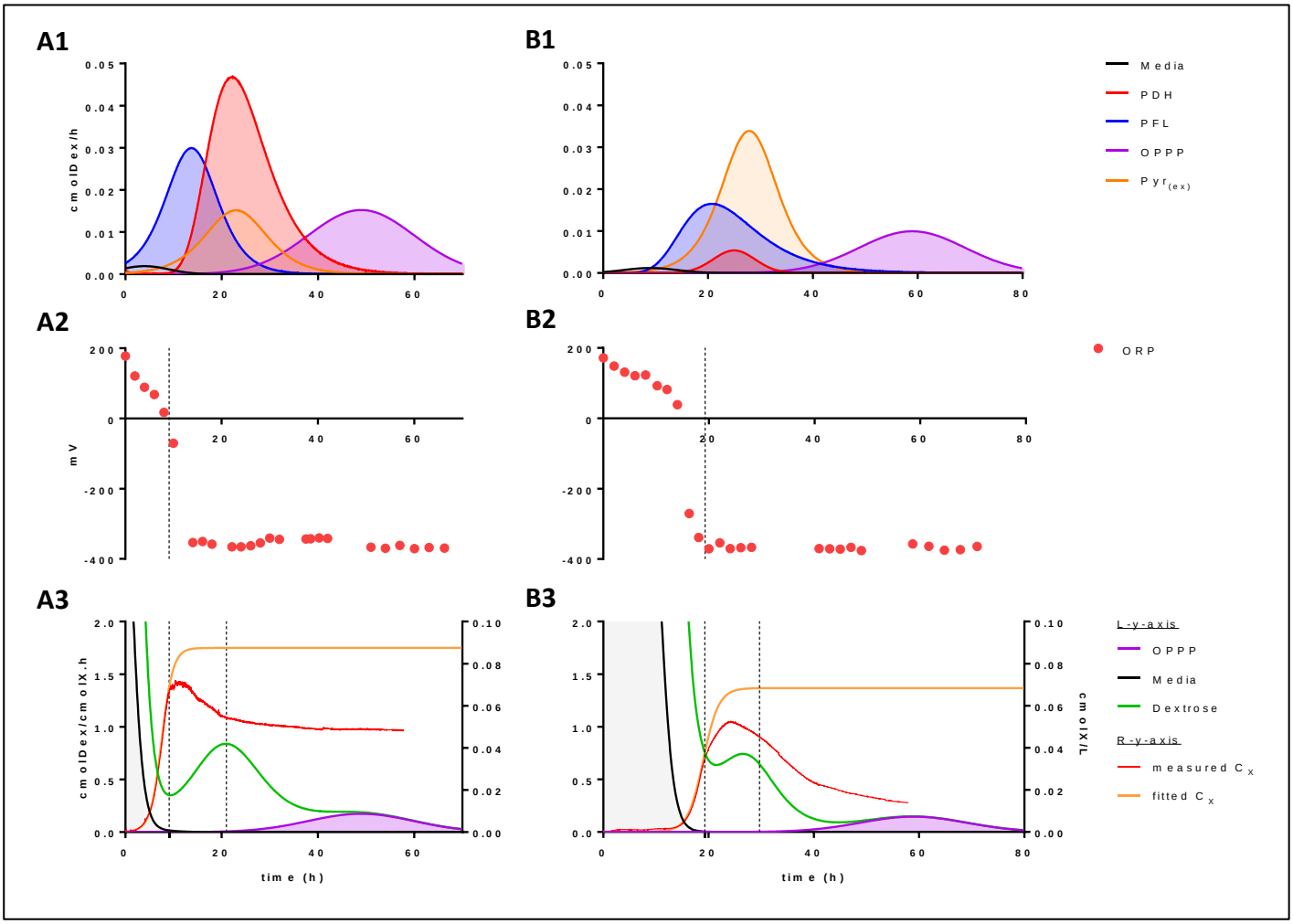

Figure 9: Volumetric dextrose consumption rate as it relates to the specific energy production pathways utilised, measured ORP data and measured and fitted biomass concentration curves

Legend: (A1, B1) Both media display preference for pathways with higher energy extraction efficiencies, sequentially substituting them for pathways with lower energy extraction efficiencies as fermentation progresses. (A2,B2) Measured ORP data. A3,B3 [left y-axis]) Depiction of cell-based dextrose consumption rates (green), and cell-based dextrose consumption rates as it relates to the media mediated (ORP) energy extraction pathway (grey) and OPPP energy extraction pathway (purple). [right y-axis]) Measured (red) and fitted (orange) biomass concentration curves; A correlation coupling the onset of flocculation to termination of the ORP energy extraction pathway is obtained.

Once redox and mass balances were confirmed, individual redox neutral energy pathway activities were established by proportioning molar volumetric rates to the above-mentioned combinatory pathways (Figure 9). By partitioning the acid production rates in their respective redox neutral pathways, a clear pattern, irrespective of the medium composition, is apparent. It is evident from the data that, except for pyruvate excretion, *A. succinogenes* successively cycles through its most (ORP: 0.667 $mol_{ATP}Cmol_{Dex}^{-1}$) to its least (OPPP: 0.452 $mol_{ATP}Cmol_{Dex}^{-1}$) efficient energy extraction route (Figures 8 and 9).

Initially, when regarding succinic acid as the sole NADH sink, the PFL route is actively producing a 1:1:1 ratio of succinic, acetic and formic acid. This is followed by a shift towards a regime in which formic acid production is omitted, resulting in a 2:1 production ratio of succinic to acetic acid. It is unclear from this data whether PFL activity is gradually replaced with PDH activity, or whether FDH activity is steadily upregulated, or there is a combination of the two mechanisms, all of which would provide the same response. For this discussion, however, it will be referred to as PDH activity.

The peak in PDH activity is correlated with a proximate peak in pyruvic acid excretion activity (Figure 9). Considering the huge difference in energy production efficiencies between the PDH and pyruvic acid excretion pathways, an argument can be made for pyruvic acid production operating primarily as an overflow mechanism to divert carbon away from acetic acid production. This argument is supported by the finding that no measurable trace of oxaloacetic acid was present, that has production pathway that would result in an energy efficiency equivalent to that of pyruvic acid production at 0.444 $mol_{ATP}Cmol_{Dex}^{-1}$. The co-activity of PDH and pyruvic acid excretion is followed by the shift towards complete OPPP activity, a homo-succinic acid production pathway (Figure 9). Of note is that *A. succinogenes* did not utilise energy production strategies that would result in lower energy production efficiencies than the OPPP could provide, such as the production of the redox neutral products ethanol, or of malic, fumaric or lactic acid, all of which result in an efficiency of 0.333 $mol_{ATP}Cmol_{Dex}^{-1}$. However, this is beneficial to the cause of succinic acid production as no carbon is lost to these additional catabolites.

Furthermore, before the onset of succinic acid production, acetic acid production was already in effect. This denotes a regime in which succinate does not act as the redox consuming counterpart. As a reduction in the overall media ORP was observed (Figure 9), it is

thought that the reduction potential is lost to, or used to condition, the aqueous environment in addition to the redox required by biomass formation (Villadsen et al., 2011; McKinlay et al., 2007) (Reaction 13).

$$nCH_2O + mNH_3 + \omega NADPH + \gamma ATP \rightarrow X + \alpha CO_2 + \beta NADH \quad ;\text{and } \omega > \beta \qquad \text{Reaction 13}$$

From an energy perspective, it conforms to the pattern of utilising more efficient routes first, as the production of acetic acid (uncoupled from an redox consuming metabolic branch) results in an efficiency of 0.667 $mol_{ATP}Cmol_{Dex}^{-1}$, which exceeds the efficiency of PFL coupled to succinate production(Figure 5).

Reduction of the media ORP was only observed to take place until the media reached an ORP of −370 mV, similar to the findings of Li et al., 2010. This indicates a ceiling that prevents *A. succinogenes* from continuously utilising the medium as an NADH sink to favour pure acetic acid production. This effect is exemplified in Li et al., 2010 where the ORP was controlled at −100 mV, bringing about a drastic shift in the ratio of acetic to succinic acid. Since the aqueous environment continuously provided a way to utilise the medium as a redox consumer, the acetic acid concentration accumulated as usual, while succinic acid production was severely suppressed. Conversely, when conditions were controlled at −350 mV, the highest ratio of succinic to acetic acid was obtained as the medium was less able to perform as a redox consuming counterpart to acetic acid production. Moreover, as indicated in Figure 9, the termination of the medium-assisted energy production pathway is closely associated with the onset of flocculation in both medium compositions, as well as with an increase in the overall cell-based dextrose consumption rates, followed by a decrease once growth terminates. This perturbation of the dextrose consumption rate witnessed is a conservative estimate as it is based on the fitted biomass curve; an even greater shift would have been apparent if the measured data had been used to calculate $CmolX^{-1}$-based rates. This phenomenon is probably explained by an increase in the energy demand for biofilm formation.

Although it is evident from this analysis that *A. succinogenes* is continually diminishing its energy extraction efficiency, it should be pointed out that the process results in lower production ratios, and eventually complete cessation of production, of first formic and then acetic acid. This may imply a mechanism in which the extracellular concentration of these acids provides enough of a stress response to induce the shutdown of their catabolic production by *A. succinogenes*. Such a mechanism becomes plausible when considering the fact that all produced catabolites must consume a fraction of the energy generated by their production for the cell to rid itself of their cytotoxic accumulation. The bi-lipid membrane remains a selective barrier preventing the transfusion of charged molecules, such as dissociated organic acids, a state in which all organic acids produced by *A. succinogenes* are at a cytosolic pH of >7.0.

Due to the limited passive diffusion achievable by the cell to rid itself of the cytotoxic build-up of these catabolites, an energy-associated transport mechanism would be required. Furthermore, due to high permeability coefficients (Walter & Gutknecht, 1986), it is plausible that formic and acetic acid may easily penetrate the bi-lipid membrane through passive back-diffusion once sufficient extracellular concentrations are reached. Theoretically, this could result in an increasing ATP cost to excrete these catabolites vs the energy gained from their production to maintain homeostasis, subsequently generating the need to shut down their production.

5 Conclusions

A. succinogenes displayed high selectivity towards utilising its most ATP efficient catabolic routes in preference to less efficient routes over the entire course of its fermentative lifespan, with the exception of pyruvate excretion, and irrespective of medium composition. This observation points to energy maximisation as a global prerequisite for the microbe's metabolic logic gates.

In addition, the peak in pyruvate excretion was found to coincide with the termination of growth, as well as being proximate to the peak of the PDH route. Due to the low energy extraction efficiency of the pyruvate excretion route, it is postulated that the activation of this route is not driven by energy gain as with the other routes, but rather by a mechanism employed by the organism to divert carbon away from the production of acetic acid. This is emphasised by the lack of measured oxaloacetic acid production, which would, in theory, result in energy efficiency similar to that of pyruvate excretion.

It is furthermore thought that by limiting acetic acid production *A. succinogenes* optimises energy extraction by preventing, or at least limiting, a runaway mechanism that could result from passive acetic acid back-diffusion and its subsequent active export to

prevent toxic build-up. Should such a mechanism be in effect and be dependent on the extracellular concentration of acetic acid, it follows that diverting carbon flux to pyruvic acid away from acetic acid to prevent its accumulation is likely to be energetically more favourable. It could be argued that the shift from the PFL to the PDH route might be due to a similar effect, but in this case with regard to formic acid, as this acid is much more likely to diffuse passively across the bi-lipid membrane (Walter & Gutknecht, 1986).

Moreover, it was found that *A. succinogenes* uses its liquid environment to its advantage to achieve an initial brief period of high energy extraction efficiency with the onset of growth, by channelling the reduction power generated through acetic acid production to the medium until its oxidative capabilities have been exhausted. This was found to be at a medium ORP of approximately −370 mV and coincided with the onset of flocculation of biomass and the initialisation of the PDH energy extraction route. This notion is supported by the findings of another independent study which observed a significant shift in product distribution when ORP was artificially maintained at less negative ORP values (Li et al., 2010).

Pure homosuccinic acid production via the OPPP pathway was also found to be active during the final stages of fermentation. This is attributed to the relatively low energy extraction efficiency of the pathway. Therefore, it may be possible to isolate this behaviour, but for *A. succinogenes* to reach this stage it must first exhaust all other, more energy-efficient, routes. Since the more efficient routes all involve the production of acetic acid from AceCoA, which is a key anabolic molecule (McKinlay et al., 2007), it may prove difficult to circumvent the co-production of acetic acid entirely.

6 References

Beauprez, J., De Mey, M. & Soetaert, W. (2010). Microbial succinic acid production: Natural versus metabolic engineered producers. *Process Biochemistry*, 45(7): 1103-1114.

Black, SD (1997). *Why has glucose to be autoclaved separately?* Available at: http://www.bio.net/bionet/mm/methods/1997-October/062161.html [accessed on 10 March 2019].

Bokranz, M., Morschel, E. & Kroger, A. (1985). Phosphorylation and phosphate-ATP exchange catalyzed by the ATP synthase isolated from *Wolinella succinogenes*. *Biochimica et Biophysica Acta*, 810: 332-339.

Bozell, J. and Petersen, G. (2010). ChemInform Abstract: Technology development for the production of biobased products from biorefinery carbohydrates – The US Department of Energy's "Top 10" Revisited. *ChemInform*, 41(28).

Bradfield, M. & Nicol, W. (2014). Continuous succinic acid production by *Actinobacillus succinogenes* in a biofilm reactor: Steady-state metabolic flux variation. *Biochemical Engineering*, 85: 1-7.

Bradfield, M. & Nicol, W. (2016). The pentose phosphate pathway leads to enhanced succinic acid flux in biofilms of wild-type *Actinobacillus succinogenes*. *Applied Microbiology and Biotechnology*, 100(22): 9641-9652.

Brink, H. & Nicol, W. (2014). Succinic acid production with *Actinobacillus succinogenes*: rate and yield analysis of chemostat and biofilm cultures. *Microbial Cell Factories*, 13(1).

Brune, A., Spillecke, J. & Kroger, A., 1987. Correlation of the turnover number of the ATP synthase in liposomes with the proton flux and the proton potential across the membrane. *Biochimica et Biophysica Acta*, 893: 499-507.

Grandviewresearch.com. (2019). *Global Maleic Anhydride Market|Industry Analysis Report, 2019-2025*. Available at: https://www.grandviewresearch.com/industry-analysis/maleic-anhydride-market [accessed on 18 September 2019].

Guettler, M., Rumler, D. and Jain, M. (1999). *Actinobacillus succinogenes* sp. nov., a novel succinic-acid-producing strain from the bovine rumen. *International Journal of Systematic Bacteriology*, 49(1): 207-216.

Hadjipetrou, L. P. & Stouthamer, A. H., 1965. Energy production during nitrate respiration by *Aerobacter aerogenes*. *Journal of General Microbiology,* 38: 29-34.

Herselman, J., Bradfield, M., Vijayan, U. & Nicol, W. (2017). The effect of carbon dioxide availability on succinic acid production with biofilms of *Actinobacillus succinogenes*. *Biochemical Engineering*, 117: 218-225.

Iverson, T. M., Luna-Chavez, C., Cecchini, G. & Rees, D. C. (1999). Structure of the *Escherichia coli* fumarate reductase respiratory complex. *Science*, 284(5422): 1961-1966.

Koshland, Jr., D. E. (2002). The Seven Pillars of Life. *Science*, 295(5563): 2215-2216.

Koushik, P., Erhardt, M., Hirano, T., Blair, D. F. & Hughes, K. (2008). Energy source of flagellar type III secretion. *Nature*, 451: 489-492.

Kroger, A., Biel, S., Simon, J., Gross. R., Unden, G. & Lancaster, C. R. (2002). Fumarate respiration of *Wolinella succinogenes*: enzymology, energetics and coupling mechanism. *Biochimica et Biophysica Acta,* 1553(1-2): 23-38.

Lancaster, C. R. D., 2003. *Wolinella succinogenes*quinol:fumarate reductase and its comparison to *E. coli* succinate: quinone reductase. FEBS Letters, 555(1): 21-28.

Lee, P., Lee, W., Lee, S. & Chang, H. (2000). Succinic acid production with reduced by-product formation in the fermentation of *Anaerobiospirillum succiniciproducens* using glycerol as a carbon source. *Biotechnology & Bioengineering*, 72(1): 41-48.

Lee, P., Lee, S., Hong, S. & Chang, H. (2002). Isolation and characterisation of a new succinic acid-producing bacterium, *Mannheimia succiniciproducens* MBEL55E, from bovine rumen. *Applied Microbiology and Biotechnology*, 58(5): 663-668.

Lemma, E., Hägerhäll, C., Geisler, V., Brandt, U., von Jagow, G. & Kröger, A. (1991). Reactivity of the *Bacillus subtilis* succinate dehydrogenase complex with quinones. *Biochimica et Biophysica Acta*, 1059(3): 281-285.

Li, J., Jiang, M., Chen, K., Ye, Q., Shang, L., Wei, P. et al. (2010). Effect of redox potential regulation on succinic acid production by *Actinobacillus succinogenes*. *Bioprocess and Biosystems Engineering*, 33(8): 911-920.

Lin, H., Bennett, G. & San, K. (2005). Fed-batch culture of a metabolically engineered *Escherichia coli* strain designed for high-level succinate production and yield under aerobic conditions. *Biotechnology and Bioengineering*, 90(6): 775-779.

Lin, S., Du, C., Koutinas, A., Wang, R. and Webb, C. (2008). Substrate and product inhibition kinetics in succinic acid production by *Actinobacillus succinogenes*. *Biochemical Engineering Journal*, 41(2), pp.128-135.

Luthfi, A., Jahim, J., Harun, S., Tan, J. and Mohammad, A. (2016). Biorefinery approach towards greener succinic acid production from oil palm frond bagasse. *Process Biochemistry*, 51(10): 1527-1537.

McKinlay, J., Zeikus, J. and Vieille, C. (2005). Insights into *Actinobacillus succinogenes* fermentative metabolism in a chemically defined growth medium. *Applied and Environmental Microbiology*, 71(11): 6651-6656.

McKinlay, J., Shachar-Hill, Y., Zeikus, J. and Vieille, C. (2007). Determining *Actinobacillus succinogenes* metabolic pathways and fluxes by NMR and GC-MS analyses of 13C-labeled metabolic product isotopomers. Metabolic Engineering, 9(2), 177-192.

McKinlay, J., Laivenieks, M., Schindler, B. et al. (2010). A genomic perspective on the potential of *Actinobacillus succinogenes* for industrial succinate production. *BMC Genomics*, 11(1): 680.

Mitchell, P. (1966). Chemiosmotic coupling in oxidative and photosynthetic phosphorylation. *Biological Reviews*, 41(3): 445-502.

Myers, J. D. & Kelly, D. J. (2005). A sulphite respiration system in the chemoheterotrophic human pathogen *Campylobacter jejuni*. *Microbiology*, 151: 233-242.

Oren, A. (1991). Anaerobic growth of halophilic archaeobacteria by reduction of fumarate. *Journal of General Microbiology*, 137: 1387-1390.

Shafiee, S. & Topal, E. (2009). When will fossil fuel reserves be diminished? *Energy Policy*, 37(1): 181-189.

Shi, L., Squier, T. C., Zachara, J. M. & Fredrickson, J. K. (2007). Respiration of metal (hydr)oxides by Shewanella and Geobacter: a key role for multihaem c-type cytochromes. *Molecular Microbiology,*65(1): 12-20.

Song, H. & Lee, S. (2006). Production of succinic acid by bacterial fermentation. *Enzyme and Microbial Technology*, 39(3): 352-361.

Villadsen, J., Nielsen, J. and Lidén, G. (2011). *Bioreaction Engineering Principles*, 3rd ed. New York: Springer.

Walter, A. & Gutknecht, J. (1986). Permeability of small nonelectrolytes through lipid bilayer membranes. *Journal of Membrane Biology*, 90(3): 207-217.

Werpy, T. & Petersen, G. (Eds). (2004). *Top Value Added Chemicals from Biomass*. Volume I. *Results of Screening for Potential Candidates from Sugars and Synthesis Gas*. National Renewable Energy Laboratory, Golden, CO, US. Available at http://www.nrel.gov/docs/fy04osti/35523.pdf.

Willey, J. M., Sherwood, L. M. & Woolverton, C. J. (2011). *Prescott's Microbiology*, 8th ed. New York: McGraw-Hill.

Zeikus, J., Jain, M. & Elankovan, P. (1999). Biotechnology of succinic acid production and markets for derived industrial products. *Applied Microbiology and Biotechnology*, 51(5): 545-552.